The opaque mineralogy of metasedimentary rocks of the Meguma Group, Beaverbank-Rawdon area, Nova Scotia

S.J. Haysom[1], R.J. Horne[2] and G. Pe-Piper[1]

[1]*Department of Geology, Saint Mary's University, Halifax, Nova Scotia B3H 3C3, Canada*
[2]*Nova Scotia Department of Natural Resources, P.O. Box 698, Halifax, Nova Scotia B3J 2T9, Canada*

Opaque mineralogy of a representative cross-section of deformed and metamorphosed turbiditic slate and metasandstone of the Meguma Group has been investigated optically and by electron microprobe. A strong stratigraphic control over the presence and abundance of certain opaque minerals is recognized, which may prove useful for environmental evaluation such as acid drainage potential. Abundant pyrite and pyrrhotite in the lower Halifax Formation reflect concentration of early diagenetic pyrite resulting from the reduction of seawater sulphate under anoxic conditions. Magnetite is restricted to the Goldenville Formation. Ilmenite and rutile occur throughout the succession, and minor chalcopyrite, arsenopyrite, covellite, hematite and glaucodot were also noted.

Pyrrhotite and ilmenite, as well as spessartine, chlorite and chloritoid porphyroblasts, developed during prograde metamorphism before and/or during cleavage formation, which also resulted in removal of early diagenetic pyrite. Later pyrite formed by replacement or remobilization of pyrrhotite during retrograde metamorphism. Colloform pyrite, arsenopyrite and chalcopyrite are the youngest mineral phases.

On a étudié la structure minéralogique opaque d'un échantillon représentatif de métagrès et d'ardoise turbiditique déformés et métamorphisés du groupe de Meguma, optiquement ainsi qu'à l'aide d'une microsonde électronique. On a ainsi reconnu un contrôle stratigraphique prononcé sur la présence et l'abondance de certains minéraux opaques, ce qui pourrait s'avérer utile pour une évaluation environnementale, comme celle du potentiel de drainage acide. Les quantités abondantes de pyrite et de pyrrhotine dans la partie inférieure de la Formation d'Halifax témoignent d'une concentration de pyrite diagénétique précoce provenant de la réduction du sulfate d'eau salée dans des conditions anoxiques. La magnétite se limite à la Formation de Goldenville. On relève la présence d'ilménite et de rutile partout dans la succession, en plus de petites quantités de chalcopyrite, d'arsénopyrite, de covellite, d'hématite et de glaucodot.

La pyrrhotine et l'ilménite, tout comme la spessartine, la chlorite et les porphyroblastes chloritoïdes, sont apparus au cours d'un métamorphisme prograde avant ou pendant la formation du clivage, qui a provoqué en plus un retrait de la pyrite diagénétique précoce. La pyrite ultérieure s'est formée par remplacement ou remobilisation de la pyrrhotine au cours d'un rétrométamorphisme. La pyrite colloforme, l'arsénopyrite et la chalcopyrite représentent les phases minérales les plus récentes.

[Traduit par la rédaction]

INTRODUCTION

The Lower Palaeozoic Meguma Group of southern Nova Scotia experienced regional deformation and greenschist to amphibolite metamorphism during the mid-Devonian Acadian Orogeny (Muecke *et al.*, 1988; Keppie and Dallmeyer, 1987). The slates and metasandstones of the Meguma Group contain a wide variety of opaque minerals and limited documentation of the opaque mineralogy has been presented previously. Black slate and associated siltstone in the basal Halifax Formation is sulphide-rich, with significant amounts of pyrite and pyrrhotite (e.g., O'Brien, 1988; Waldron, 1992; Horne, 1995; Knee, 1995). The manganiferous beds underlying the black slates also generally host considerable amounts of sulphides, including pyrrhotite and pyrite, and locally chalcopyrite, sphalerite, arsenopyrite and galena (Binney *et al.*, 1986; Jenner, 1982; MacInnis, 1986). This unit also contains ilmenite and rutile (Binney *et al.*, 1986). Schwarz and Broom (1994) used Curie temperatures to determine that pyrrhotite was present in the Halifax Formation and magnetite in the Goldenville Formation. King (1994) documented pyrite and pyrrhotite in the Halifax Formation and magnetite in the Goldenville Formation. Further study by King (1995), employing semi-quantitative electron microprobe analysis of magnetic fractions of the samples used in this paper, determined variable concentrations of pyrite, pyrrhotite, ilmenite, magnetite, and rutile.

In this study, we have investigated, using the electron microprobe, the types of opaque minerals present in a representative section of the Meguma Group, extending from the upper Goldenville Formation to the upper Halifax Formation. We have determined the paragenesis of these minerals in relation to the depositional, structural and metamorphic history of the Meguma Group. This study provides

information on the type and distribution of opaque minerals in the Meguma Group which is important for environmental assessment, including evaluation of acid drainage resulting from oxidation of sulphide minerals.

Geology of the Meguma Group

The Meguma Group represents a turbiditic succession subdivided into the lower sandstone-dominated Goldenville Formation and the overlying shale-dominated Halifax Formation (Fig. 1) (Fletcher and Faribault, 1911; Woodman, 1904; Keppie, 1979). More recently, further stratigraphic subdivision has been locally recognized, particularly in the transition zone between the Goldenville and Halifax formations and within the Halifax Formation (e.g., Binney *et al.*, 1986; O'Brien, 1988; Waldron, 1992; Schenk, 1991; Horne, 1993, 1995; Ryan, 1994; Ryan *et al.*, 1996). Sparseness of detailed mapping and variation in units does not allow for confident regional correlation at the member level. However, comparison of various areas indicates the following conformable lithologic sequence: (1) lower, undivided Goldenville Formation consisting mainly of thick-bedded metasandstone with minor slate; (2) upper Goldenville Formation comprising medium- to thin-bedded metasandstone, metasiltstone and minor slate; (3) lowermost Halifax Formation consisting of manganiferous metasiltstone/slate and including anomalous base metal concentrations locally (Binney *et al.*, 1986; Zentilli *et al.*, 1986); (4) black, graphitic, sulphide-rich slate; (5) upper Halifax Formation consisting of pale grey to green, planar to cross-laminated slate and metasiltstone. The distinctive black slate unit (4) of the Halifax Formation is recognized throughout the Meguma Group and provides a lithostratigraphic marker horizon. This stratigraphic succession represents a systematic change in depositional environment from submarine fan turbidites (Goldenville Formation) to shales formed under oceanic anoxia (manganiferous and black, sulphide-rich slates) to a shallowing through a prograding wedge of fine grained sediment (Schenk, 1991; Waldron, 1992). All components of this generalized stratigraphy are represented within the study area and are discussed further below.

Kilometre-scale, open to tight non-cylindrical folds and associated cleavage dominate the structure of the Meguma Group. Henderson *et al.* (1986) proposed a structural history which involved pre-folding cleavage development during homogenous shortening, followed by flexural shear folding (homogeneous bedding-parallel shear). Henderson *et al.* (1986), Wright and Henderson (1992) and Fueten (1984) proposed that cleavage strain reflects large volume loss (up to 60%), with little to no extension indicated. Challenges to the arguments for prefolding cleavage formation (Treagus, 1988; Williams *et al.*, 1995) and volume loss during cleavage formation (Erslev and Ward, 1994) have been presented, and therefore the relative timing of cleavage formation and folding and the method of cleavage formation are considered to be unresolved. Horne and Culshaw (1994a, 1994b) demonstrated
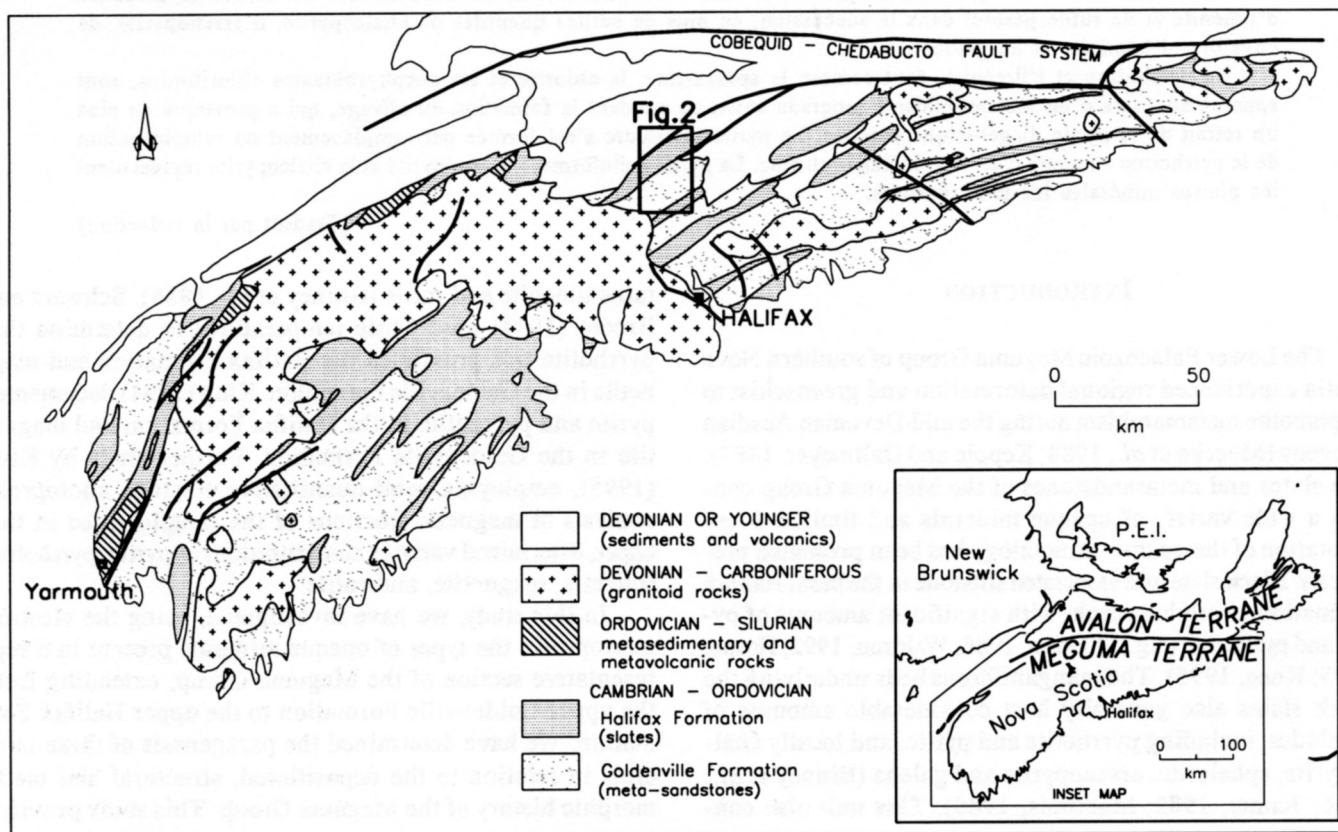

Fig. 1. Simplified geological map of the Meguma Terrane, showing basic subdivision of the Meguma Group (modified after Keppie, 1979) and the location of the study area.

that flexural-slip folding (slip on bedding-parallel planes) was, at least locally, an important folding mechanism.

GEOLOGY OF THE BEAVERBANK-RAWDON AREA

Stratigraphy

Samples for this study were collected in the Beaverbank-Rawdon area (Figs. 1, 2), 40 km north of Halifax. In this area, the Goldenville Formation is exposed in the cores of a series of anticlines and the Halifax Formation is exposed in two narrow belts in the Rawdon and Uniacke synclines. Recent mapping (Horne, 1993, 1995; Ryan, 1994; Ryan et al., 1996; Fox, 1994) has established further stratigraphic subdivision of the Goldenville and Halifax formations (Fig. 2) and a composite stratigraphic column for the area is shown in Figure 3. Samples were collected from all the exposed stratigraphic units along roads (Fig. 2).

Local subdivision of the Goldenville Formation in the area has been proposed by Ryan et al. (1996). However, this subdivision is tentative and requires further testing before stratigraphic significance can be determined. For the purposes of this paper, we leave the Goldenville Formation largely undivided. It consists primarily of massive, thickly bedded metasandstone with minor interbedded metasiltstone and slate (Fox, 1994; Ryan, 1994). The uppermost part of the Goldenville Formation is referred to as the Steves Road unit (Figs. 2, 3) and differs from the underlying section in containing a higher proportion of interbedded slate (Ryan, 1994).

In the study area the Halifax Formation has been subdivided into three units (Figs. 2, 3). The basal Beaverbank unit (Ryan et al., 1996) consists of manganese-rich slate and metasiltstone (Ryan, 1994; Ryan et al., 1996; Feetham et al., 1997). This unit is restricted to the Uniacke Syncline where it has been subdivided into the "lower beds" and "upper beds" by Ryan (1994) (Figs. 2, 3). The lower beds consist of interbedded fine grained metasandstone and silty slate, whereas the upper beds consist of Mn-rich slate, metasiltstone, fine grained metasandstone and local tightly buckled coticule horizons (i.e., spessartine-rich layers). The Cunard unit overlies the Beaverbank unit and consists of dark, locally graphitic slate and minor thin metasiltstone beds. This unit was previously referred to as the Rawdon unit in the study area (e.g., Horne, 1995; Ryan et al., 1996) and occurs in both the Rawdon and Uniacke synclines (Fig. 2). The lower part of the Cunard unit (subunit a) is characterized by abundant coarse sulphide minerals, including pyrrhotite elongate parallel to cleavage in the slate and pyrrhotite disseminations in the metasiltstone, and pyrite as cubes and veinlets. The upper part of the Cunard unit (subunit b) is lithologically similar but lacks abundant sulphide minerals. The Glen Brook unit overlies the Cunard unit in the Rawdon Syncline (Fig. 2) and consists of pale grey-green, distinctly banded, strongly cleaved metasiltstone. Visible sulphide minerals are rare in the Glen Brook unit.

Structure and metamorphism

F1-folds and cleavage

Regional (kilometre-scale) folds (F_1) dominate the structure of the area (Fig. 2) and control the stratigraphic level of exposure. The Halifax Formation is exposed in the Rawdon and Uniacke synclines in the northern and southern parts of the area, respectively. The Mount Uniacke - Renfrew and Rawdon Mines anticlines dominate the Goldenville Formation (Fig. 2). Minor (decimetre-scale) and parasitic (centimetre-scale) folds are common in the Halifax Formation, particularly in the Glen Brook unit, and are related to the regional-scale folds by a common axial-planar cleavage. The Halifax Formation is characterized by a well developed slaty cleavage, whereas cleavage in the Goldenville Formation is lacking or defined by a poorly developed spaced cleavage. The metamorphic conditions in the the area reached greenschist facies (Keppie and Muecke, 1979).

Petrographic examination of samples from the Rawdon Syncline indicates that slaty cleavage is characterized by penetrative alignment of fine grained phyllosilicates and (pressure solution) cleavage zones (Fig. 4). On the basis of texture, sulphide minerals appear to be of metamorphic origin and are described in detail below. In addition, porphyroblasts of chlorite and locally chloritoid are common to abundant in units of the Rawdon Syncline, particularly within the Glen Brook unit. The porphyroblasts locally appear to truncate the penetrative cleavage; however, cleavage zones invariably wrap around the porphyroblasts (Fig. 4) and nowhere are porphyroblasts observed to crosscut cleavage zones, thus indicating a pre- to syn-cleavage origin for the porphyroblasts. Pressure shadows filled with quartz and/or mica associated with the porphyroblasts demonstrate considerable shear strain parallel to cleavage. Symmetrical shape fabrics defined by the pressure shadows suggest a predominance of pure shear. Field observations indicate that the stretching lineation defined by the pressure shadows, as seen on cleavage, is down dip, consistent with strain associated with cleavage formation during flexural folding. Alternatively, this strain, or a component of it, may be related to Carboniferous deformation discussed below. Quartz-filled pressure shadows are also common adjacent pyrite and pyrrhotite.

Post F-1 deformation

Several post-folding structures have been recognized in the area. The northern margin of the Rawdon Syncline is overprinted by intense Carboniferous deformation, reflected in mesoscopic folding (F_2) of bedding and slaty cleavage, local development of a crenulation cleavage (S_2), bedding-parallel faults and steeply dipping brittle faults (Horne, 1993, 1995, and unpublished data). This deformation is also reflected in the adjacent Carboniferous rocks and may be re-
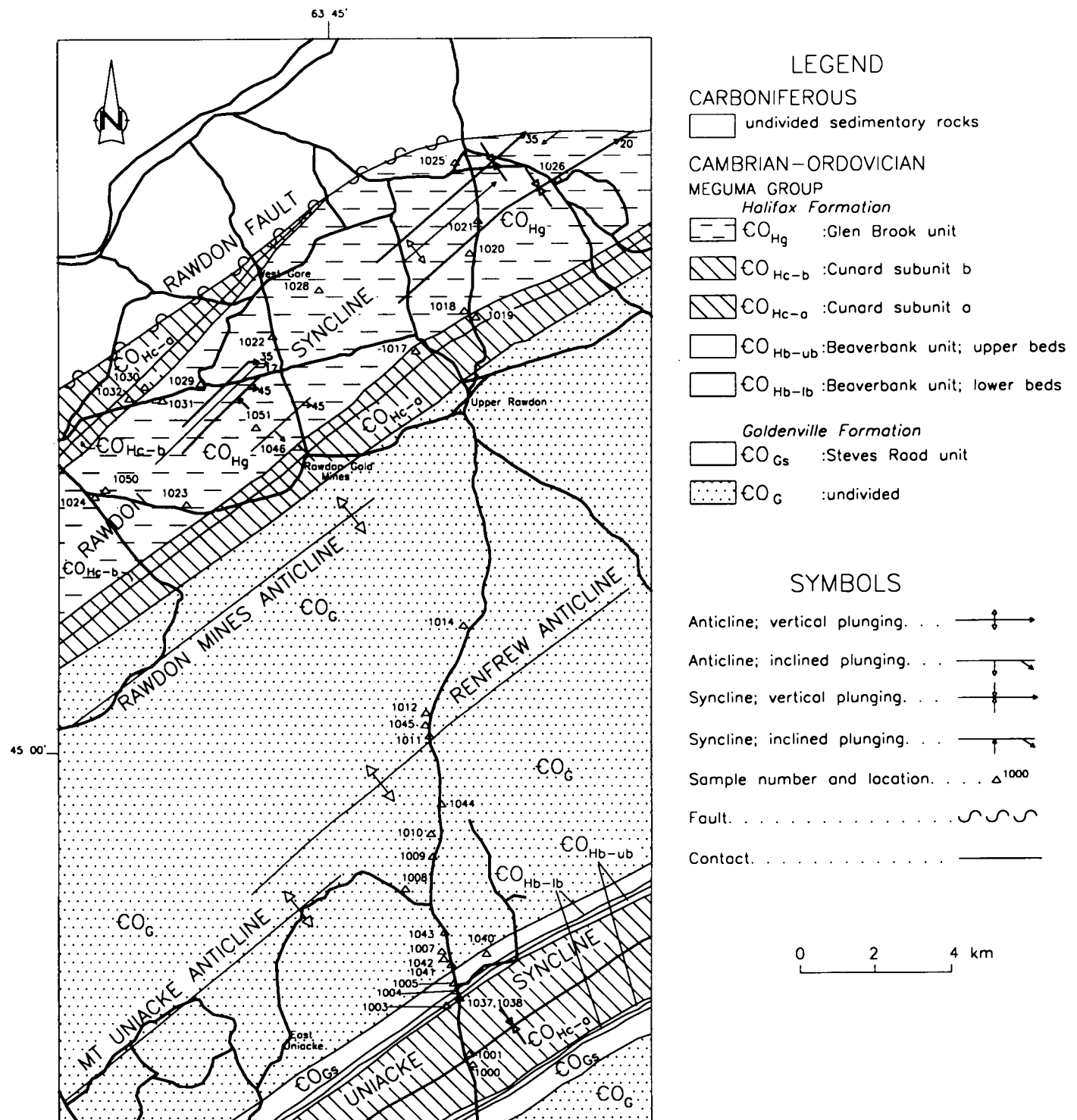
Fig. 2. Detailed geology map of the Beaverbank-Rawdon area (compiled from Horne, 1993, 1995, and Ryan, 1994) showing the location of samples.

lated to movement on the Rawdon Fault (Fig. 2). North-west-trending, generally steeply plunging, kink folds and related faults are common throughout the area, particularly in the Halifax Formation. Development of metamorphic sulphide minerals during this deformational phase is discussed below.

MINERALOGY AND GEOCHEMISTRY

Methods

Forty-one samples representing the entire stratigraphic section, from undivided Goldenville Formation to the Glen Brook unit, were studied in polished thin section. Samples

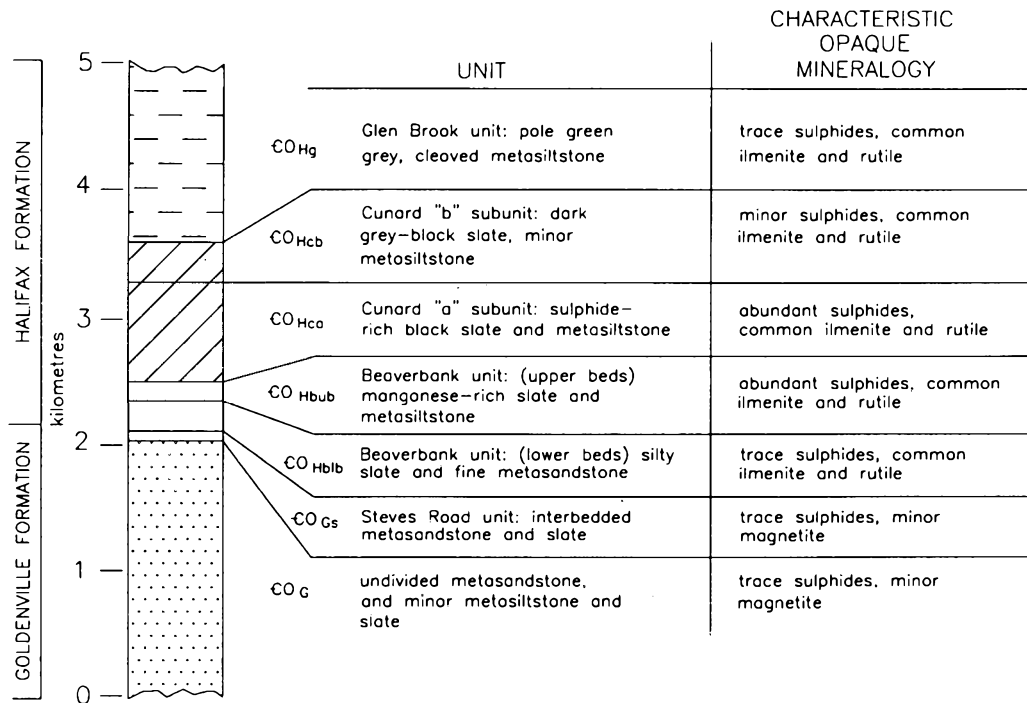| UNIT		CHARACTERISTIC OPAQUE MINERALOGY
€O Hg	Glen Brook unit: pole green grey, cleoved metosiltstone	trace sulphides, common ilmenite and rutile
€O Hcb	Cunard "b" subunit: dark grey–block slate, minor metosiltstone	minor sulphides, common ilmenite and rutile
€O Hca	Cunard "a" subunit: sulphide–rich block slate and metosiltstone	abundant sulphides, common ilmenite and rutile
€O Hbub	Beaverbank unit: (upper beds) manganese–rich slate and metosiltstone	abundant sulphides, common ilmenite and rutile
€O Hblb	Beaverbank unit: (lower beds) silty slate and fine metasandstone	trace sulphides, common ilmenite and rutile
€O Gs	Steves Road unit: interbedded metasandstone and slate	trace sulphides, minor magnetite
€O G	undivided metasandstone, and minor metosiltstone and slate	trace sulphides, minor magnetite

Fig. 3. Simplified stratigraphic log outlining the lithology and character of opaque phases for each of the units. Stratigraphic thickness of units is estimated from constructed cross-sections of Faribault (1908), Fletcher and Faribault (1905) and Horne (1993).
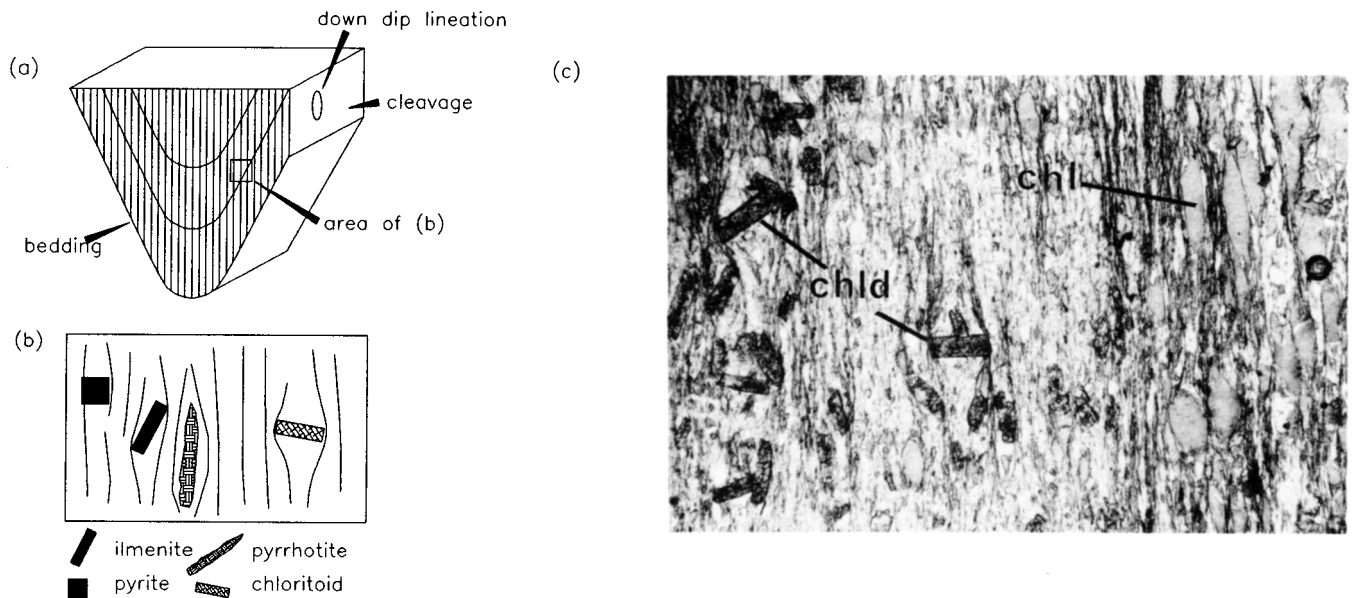

Fig. 4. (a) Schematic diagram of a cross-section of the Rawdon Syncline showing relation of cleavage and down-dip lineation on cleavage (reflecting pressure shadows on porphyroblasts) to the fold. (b) Schematic diagram of area of inset in (a) showing relation of cleavage to various mineral phases. (c) Photomicrograph of the Glen Brook unit showing relationship of cleavage to chloritoid (chld) and chlorite (chl) porphyroblasts. Cleavage zones wrap around these porphyroblasts and pressures shadows are well developed, indicating early- to syn-cleavage formation of chlorite and chloritoid.

with evidence of surficial weathering were avoided. Opaque mineralogy for each sample was identified optically and estimates of the percentage of each phase determined using standard percentage charts (Table 1). Only slate was sampled from the Halifax Formation, whereas both slate and metasandstone were sampled from the Goldenville Formation. Representative electron microprobe analyses of mineral phases are given in Tables 2 to 9. Chemical analyses of minerals were made using a JEOL-733 electron microprobe with four wavelength spectrometers and a Tracor Northern 145-eV energy-dispersive detector. Standards of known composition were used for control.

Gross stratigraphic variation in opaque mineralogy

The opaque mineralogy of the samples is summarized in Table 1. Abundance of certain minerals varies with stratigraphy, as summarized in Figure 3. Anomalous concentra-

Table 1. Abundance[1] of minerals[2] in metasedimentary rocks of the Meguma Group in the Beaverbank-Rawdon area.

Sample	Lithology	Po	Py	Cpy	Aspy	Ilm	Rt	Other Minerals
Halifax Formation								
Glen Brook								
MS1018	silty slate	T	T	T		C	C	
MS1020	slate						R	chlt(A)
MS1021	slate						R	chl(A)
MS1022	,slate						R	chlt/chl(A)
MS1023	slate					C	R	chl(A)
MS1024	slate					A	R	chl(C)
MS1025	slate					A		chl/chlt(A)
MS1026	slate					R	R	chlt(A)
MS1028	slate					T		chlt(A)
MS1029	slate					C		chl(A)
MS1031	slate					R	R	chl(A)
MS1034	slate		T				R	chl(C)
MS1050	slate					A		chl(A)
MS1052	slate		T			A	R	chl(C), hematite
Cunard "b"								
MS1017	slate					R	R	
MS1019	slate		T			A	A	chl(A)
MS1030	slate					A	A	chl(C)
MS1032	slate		T	T			A	chl(A), covellite
MS1046	slate	A	R				R	
Cunard "a"								
MS1000	slate	A	R	R			R	
MS1001	slate	A	A				R	
Beaverbank unit, upper beds								
MS1003	silty slate	A		R		A		gt(A), glauc(R)
MS1037	silty slate	A	A	T			R	
MS1038	slate		A					
Beaverbank unit, lower beds								
MS1004	slate					A	A	
Goldenville Formation								
Steve's road								
MS1005	wacke						C	mt(R), sphene
MS1006	wacke	T	T	T			T	
MS1040	wacke							sphene
MS1041	siltstone		T	T				
undivided								
MS1007	argillite			T		T		mt(T)
MS1008	wacke					C	C	
MS1009	wacke		T	T			R	cobaltite
MS1010	wacke					R	R	
MS1011	wacke		T					mt(C),hematite
MS1012	slate	A	A	R	R		C	gt(C), hematite(R)
MS1014b	wacke							mt(A)
MS1042	wacke	T	T	T				arsenopyrite
MS1043	wacke						C	mt(R),sphene
MS1044	argillite		T				R	
MS1045	wacke							mt(A)

Note:
[1]A = abundant >5%; C = common 1-5%; R = rare <1%; T = trace
[2]Po = pyrrhotite; Py = pyrite; Cpy = chalcopyrite; Aspy = arsenopyrite; Ilm = ilmenite; Rt = rutile; gt = garnet; chl = chlorite; chlt = chloritoid; mt = magnetite; glauc = glaucodot

tions of pyrite and pyrrhotite characterize the Cunard unit, consistent with the regional character of black slates of the Halifax Formation throughout the Meguma terrane. Pyrite and pyrrhotite are also common in the Beaverbank unit. Magnetite occurs only in metasandstone of the Goldenville Formation. No apparent correlation can be made between stratigraphy and the occurrence of ilmenite or rutile. The Glen Brook unit is characterized by low abundance of opaque minerals.

Sulphide minerals

Pyrrhotite

Pyrrhotite is abundant (commonly up to 10%) within the Cunard unit and the upper beds of the Beaverbank unit, although not in every sample. Grains range from 1 mm to 1 cm in length. Minor pyrrhotite in two metasandstone samples from the Goldenville Formation (Table 1) occurs as randomly distributed, subhedral grains approximately 1 mm in length. When viewed under crossed nicols, the pyrrhotite of the slates is noticeably polycrystalline, especially around grain boundaries. Based on the relationship of pyrrhotite to cleavage, two generations (1, 2) can be distinguished. Both occur as elongate, disseminated xenomorphic masses oriented parallel to cleavage.

Generation 1: Pressure shadows are visible adjacent to most first generation pyrrhotite and cleavage wraps around the pyrrhotite grains. Some grains are boudinaged parallel to cleavage with quartz filling extensional fractures perpendicular to cleavage. This extension likely parallels the down-dip lineation noted for the chlorite and chloritoid porphyroblasts in the Glen Brook unit, thus reflecting extension during folding and cleavage development. These observations indicate that, like chlorite and chloritoid, this generation of pyrrhotite formed prior to or during cleavage development. Garnet porphyroblasts of spessartine composition in two thin sections from the upper beds of the Beaverbank unit were formed in association with pyrrhotite grains, either as single crystals containing pyrrhotite, or as a group of juxtaposed garnet crystals surrounding a large pyrrhotite grain (Fig. 5a). This mode of occurrence of garnet supports early formation of pyrrhotite. Slight fracturing of garnet perpendicular to cleavage is common and presumably reflects the same down-dip extension discussed above, indicating a pre- to syn-cleavage origin for garnet also.

Fig. 5. Selected photomicrographs in reflected light showing opaque mineral assemblages. (a) Sample MS1003-2 (slate). Pyrrhotite (bronze) with glaucodot (white) surrounded by garnet (var. spessartine) (clear grey) (f.o.v. 4 mm). (b) Sample MS1001-4 (slate). Muscovite (dark grey/blue) oriented parallel to cleavage within second generation pyrrhotite (brown) (f.o.v. 0.5 mm). (c) Sample MS1012-5 (slate). Pyrrhotite (white/gold), and partial replacement by colloform pyrite (yellow/gold) (f.o.v. 4 mm). (d) Sample MS1000-1 (slate). Pyrrhotite (gold), and initial replacement of birds-eye texture pyrite along grain boundaries and internal cracks (f.o.v. 4 mm). (e) Sample MS1038-1 (slate). Pyrite cubes (gold) overprinting cleavage. Grainy pyrite in right corner was probably formerly a pyrrhotite grain, now completely replaced by pyrite (gold) and quartz (clear grey) (f.o.v. 4 mm). (f) Sample 1012-8 (slate). Arsenopyrite (white) in colloform pyrite (gold). Note the inclusion of pyrrhotite (light brown) within the arsenopyrite crystal, a replacement relict (f.o.v 0.5 mm). (g) Sample MS1003-4 (slate). Chalcopyrite (gold) and glaucodot (white), an orthorhombic euhedral crystal, inside a pyrrhotite grain (brown), surrounded by a corona of juxtaposed garnet crystals (grey) (f.o.v. 1 mm). (h) Sample MS1003 (slate). Ilmenite crystals (white laths) oriented parallel to cleavage. Garnet crystals (clear grey) with some inclusions of ilmenite (arrow) (f.o.v. 4 mm).
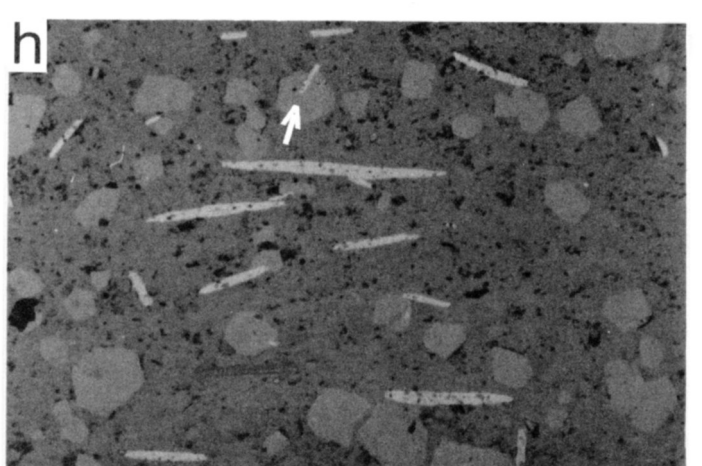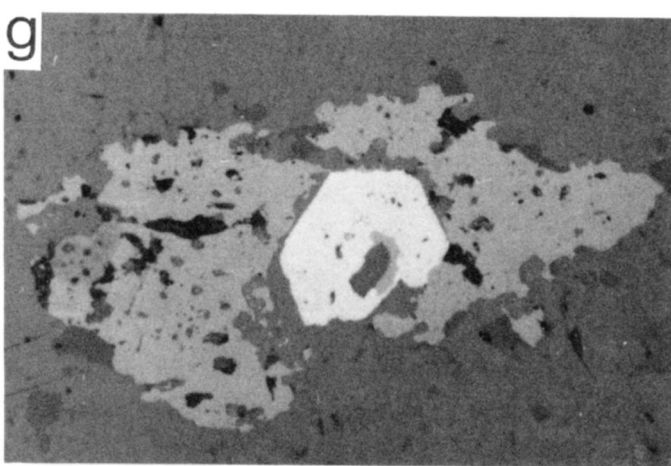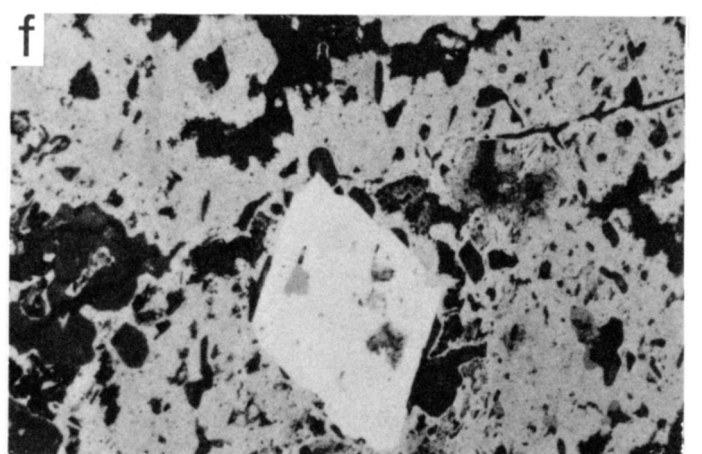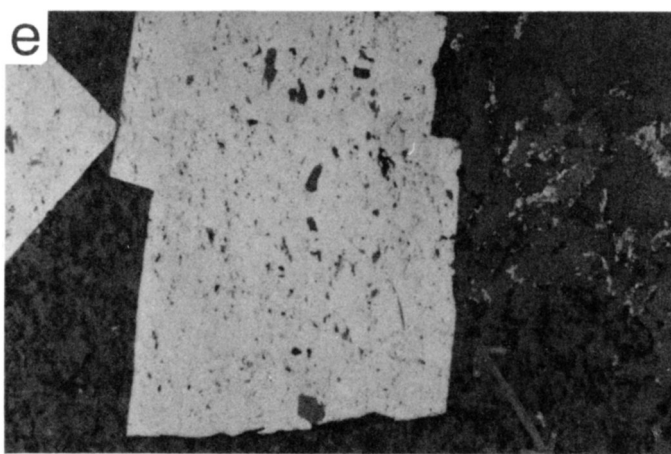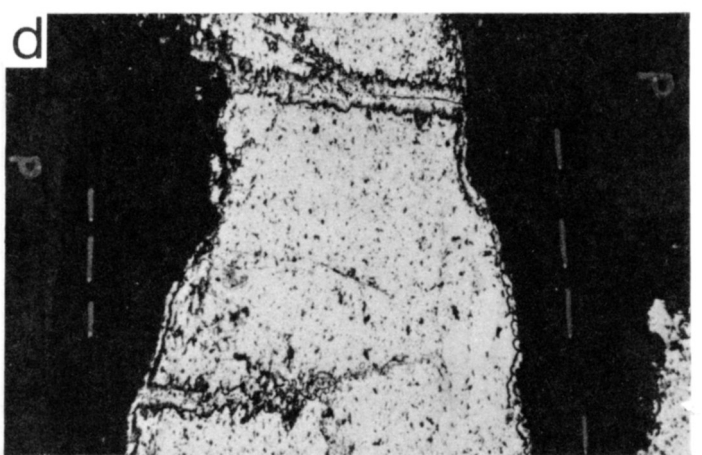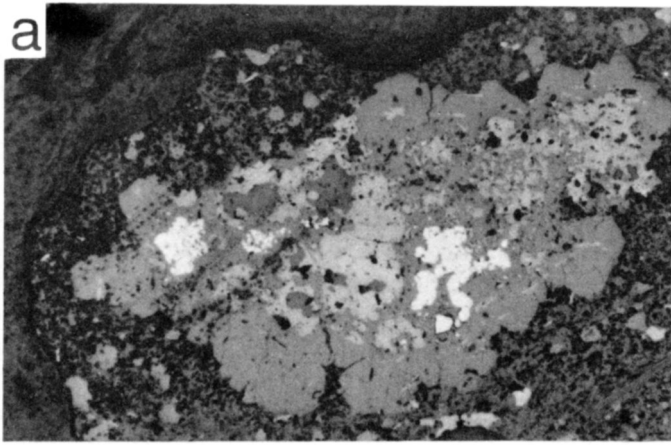
Generation 2: A second generation of pyrrhotite formed contemporaneously with, or after, cleavage. Evidence for the second generation of pyrrhotite is the occurrence of muscovite grains within a pyrrhotite grain which are parallel to cleavage (Fig. 5b). This indicates that this generation of pyrrhotite could not have grown prior to the cleavage represented by the muscovite inclusions. Other evidence is overprinting of cleavage by pyrrhotite grains. The second generation of pyrrhotite is otherwise indistinguishable from the first, as most second generation pyrrhotite has the same morphology, and is preferentially oriented parallel to cleavage.

Some pyrrhotite grains are unaltered; however, most grains are partially or entirely replaced by colloform or bird's-eye pyrite or marcasite (Fig. 5c,d), giving a skeletal appearance. Alteration is everywhere stronger in grains where surrounding cleavage planes are large and well defined.

The two generations of pyrrhotite cannot be distinguished geochemically, ranging in atomic percentage of iron from 45.65 to 46.70% ($FeO_{0.84}S_1$ to $Fe_{0.88}S_1$) (Table 2), with a mean formula of $Fe_{0.87}S_1$. Compositions range from approximately Fe_6S_7 to Fe_7S_8.

Pyrite

Pyrite is abundant in the Cunard unit and the upper beds of the Beaverbank unit, comprising up to 8% of the rock. In contrast, only a few metasandstone samples from the Goldenville Formation contain pyrite, with abundances of less than 1%. The pyrite is of two types: one type resulted from the replacement of pyrrhotite, and the other occurs as isolated, subhedral to anhedral, inclusion-free grains.

Type 1: Pyrite resulting from the alteration of pyrrhotite has two distinct habits: colloform (Fig. 5c) and birds-eye texture (Fig. 5d). Some altered grains are tarnished and it is difficult to distinguish their habit (tarnished samples were not analysed by electron microprobe). This type of pyrite is particularly common in strongly cleaved slates with well-developed cleavage planes, which would have facilitated infiltration of a fluid. Partial alteration occurs along grain boundaries, cleavage openings, and fractures in the pyrrhotite. Alteration includes the formation of pyrite stringers which branch off the altered pyrrhotite grains along cleavage planes.

Type 2: Type 2 pyrite is characterized by coarse cubes (Fig. 5e) which typically appear to overprint cleavage. However, locally cleavage is slightly wrapped around this pyrite and quartz "beards" are developed indicating cleavage-parallel strain postdating the pyrite. These observations suggest a late- to post-cleavage origin for this type of pyrite. This pyrite is observed in some Goldenville metasandstone samples as random cubic grains, <2 mm in width. Pyrite crystals of

Table 2. Representative electron microprobe analyses of pyrrhotite.

Sample No.	MS1000	MS1000	MS1000	MS1003	MS1012	MS1006	MS1006
Unit	Cunard a	Cunard a	Cunard a	Beav(ub)[1]	Gold.[2]	Steves Rd.	Steves Rd.
Lithology	Slate	Slate	Slate	Silty Slate	Slate	wacke	wacke
Position	1-19	2-29	3-9	2C	4-48	1A	1C
wt.%							
Fe	60.59	59.58	59.55	59.79	59.25	60.61	60.32
S	39.76	39.82	39.81	39.69	39.33	39.19	39.07
As	-	-	0.25	0.24	0.16	-	0.24
Ni	-	-	-	0.53	0.13	0.29	-
Co	-	-	-	0.34	0.29	-	-
W	-	-	0.30	0.29	0.32	0.24	0.26
Total	100.35	99.40	99.91	100.88	99.48	100.33	99.89
at.%							
Fe	46.66	46.21	46.10	45.98	46.15	46.89	46.89
S	53.34	53.79	53.69	53.18	53.37	52.83	52.91
As	-	-	0.14	0.15	0.09	-	0.14
Ni	-	-	-	0.39	0.10	0.22	-
Co	-	-	-	0.25	0.22	-	-
W	-	-	0.07	0.07	0.08	0.06	0.06
Total	100.00	100.00	100.00	100.00	100.00	99.99	100.00
Formula							
Fe	0.88	0.86	0.86	0.87	0.87	0.89	0.89
S	1.00	1.00	1.00	1.00	1.00	1.00	1.00
Total	1.88	1.86	1.86	1.87	1.87	1.89	1.89

[1]Beav(ub) = upper beds of the Beaverbank unit
[2]Gold. = Goldenville Formation

this type may also have long pyrite stringers extending up to 4 cm (0.1 mm thick) along cleavage planes, that may be attributed to mobilization of fluid along cleavage fractures.

A slate sample from the Beaverbank unit displays features which may indicate a possible relationship between the two types of pyrite. In this sample, Type 1 pyrite resulted from the complete replacement of pyrrhotite, with subsequent replacement of this Type 1 pyrite by quartz resulting in a skeletal texture (Fig. 5e). Pyrite stringers which extend from adjacent Type 2 pyrite are interpreted to reflect remobilization of type 1 pyrite during replacement by quartz to form the Type 2 pyrite.

All pyrite analyses show consistent stoichiometric ratios as FeS_2. Elements other than iron make up ≤ 1.4 atomic % (Table 3). Nickel reaches a maximum atomic % of 1.17, and cobalt 0.52%. Variation in single crystals of up to 1% (atomic) nickel does not indicate another generation of pyrite, only enrichment during crystallization.

Sulpharsenides

Arsenopyrite was found in two samples from the Goldenville Formation, glaucodot was observed in the Beaverbank unit

and cobaltite was noted in a sample from the Goldenville Formation.

Arsenopyrite occurs as euhedral, idioblastic crystals of arsenopyrite within Type 1 pyrite (Fig. 5f) in a metasandstone sample (MS-1042), and hosts inclusions of pyrrhotite interpreted as replacement relicts. Ramdohr (1980) described similar inclusion relicts in other arsenopyrite occurrences. The above relationships indicate that arsenopyrite postdated pyrrhotite, but predated pyrite in this sample. The arsenopyrite has low totals of arsenic, below the stoichiometric composition, which is likely due to vacancies at As positions in the lattice.

Arsenopyrite from a slate sample (MS-1012) contains anomalous amounts of cobalt (≤ 3.08 wt.%, Table 4). The inverse relationship between Co and Fe (Table 4) suggests replacement of Fe by Co. The mean calculated formula from microprobe data is $Fe_{0.935}Co_{0.081}As_{0.980}S$, which chemically is FeAsS. Ramdohr (1980) noted that arsenopyrite always contains some amount of Co, which may be as high as Fe/Co=2/1. Stoichiometric totals plot near the FeAsS apex, in the NiAsS-CoAsS-FeAsS ternary system, for the metasandstone sample and with a slight CoAsS component for the slate sample (Fig. 6). This indicates little to no contamination of the arsenopyrite by metals with similar sized ions (i.e., Co, Ni).

Table 3. Representative electron microprobe analyses of pyrite.

Sample No.	MS1012	MS1001	MS1001	MS1000	MS1009	MS1009	MS1041
Unit	Gold.[1]	Cunard a	Cunard a	Cunard a	Gold.	Gold.	Steves Rd.
Lithology	Slate	Slate	Slate	Slate	wacke	wacke	wacke
Position	1-53	4A1	4B	3-10	2B	2C	3-67
wt.%							
Fe	45.59	46.25	46.97	46.33	44.28	47.42	42.83
S	52.20	53.21	54.20	52.93	53.82	53.88	51.37
As	0.17	0.25	0.20	-	-	-	0.23
Ni	0.13	0.94	-	-	1.47	-	0.71
Cu	-	-	-	-	-	-	1.20
Zn	-	-	-	-	-	-	0.30
Co	0.47	-	-	-	-	-	0.25
W	0.30	-	0.26	-	0.33	0.23	0.30
Total	98.86	100.65	101.63	99.26	99.90	101.53	97.19
at.%							
Fe	33.20	33.03	33.17	33.44	31.74	33.55	31.77
S	66.22	66.20	66.67	66.56	67.19	66.40	66.39
As	0.09	0.14	0.11	-	-	-	0.13
Ni	0.90	0.64	-	-	1.00	-	0.50
Cu	-	-	-	-	-	-	0.78
Zn	-	-	-	-	-	-	0.19
Co	0.33	-	-	-	-	-	0.17
W	0.07	-	0.06	-	0.07	0.05	0.07
Total	100.00	100.00	100.00	100.00	100.00	100.00	100.00
Formula							
Fe	1.00	1.00	1.00	1.01	0.95	1.01	0.96
S	2.00	2.00	2.00	2.00	2.00	2.00	2.00
Total	3.00	3.00	3.00	3.01	2.95	3.01	2.96

[1]Gold. = Goldenville Formation

Table 4. Representative electron microprobe analyses of arsenopyrite.

Sample No.	MS1012	MS1012	MS1042	MS1042
Unit	Gold.[1]	Gold.	Gold.	Gold.
Lithology	Slate	Slate	wacke	wacke
Position	80-60	80-62	3-73	3-77
wt.%				
Fe	31.98	31.52	34.31	33.84
As	44.59	44.61	42.90	44.10
S	19.39	19.56	20.25	20.05
Ni	-	-	-	0.31
Co	2.73	3.08	-	0.17
Sb	0.16	0.25	-	-
Zn	-	-	-	0.47
W	0.18	-	-	0.23
Total	99.03	99.02	97.46	99.17
at.%				
Fe	31.44	30.86	33.78	32.99
As	32.67	32.56	31.49	32.05
S	33.24	33.37	34.73	34.05
Ni	-	-	-	0.29
Co	2.55	2.86	-	0.16
Sb	0.07	0.14	-	-
Zn	-	-	-	0.39
W	0.06	-	-	0.07
Total	100.00	100.00	100.00	100.00
Formula				
Fe	0.95	0.92	0.97	0.97
As	0.98	0.98	0.91	0.94
S	1.00	1.00	1.00	1.00
Total	2.93	2.90	2.91	2.91

[1]Gold. = Goldenville

Solid solution is extensive between FeAsS, CoAsS, and NiAsS, and between the numerous arsenides within this system, and optical identification is the most reliable method which can be used to define the different mineralogy. Fe-As-Co mineral phase boundaries are undefined, and overlap, making mineral identification based on microprobe data alone impossible. Numerous polycrystalline aggregates (Fig. 5a) and euhedral to subhedral crystals (Fig. 5f) of glaucodot have been identified optically and by electron microprobe (Table 5; Fig. 6) in a slate sample (MS-1003) from the upper beds of the Beaverbank unit. The analyzed sample contains anomalous amounts of Ni (Table 5) and the calculated chemical formula ranges from $(Co,Fe,Ni)_{0.88}As_{0.83}S$ to $(Co,Fe,Ni)_{0.96}As_{0.99}S$. Ramdohr (1980) described glaucodot as mixed crystals of the arsenopyrite series containing more
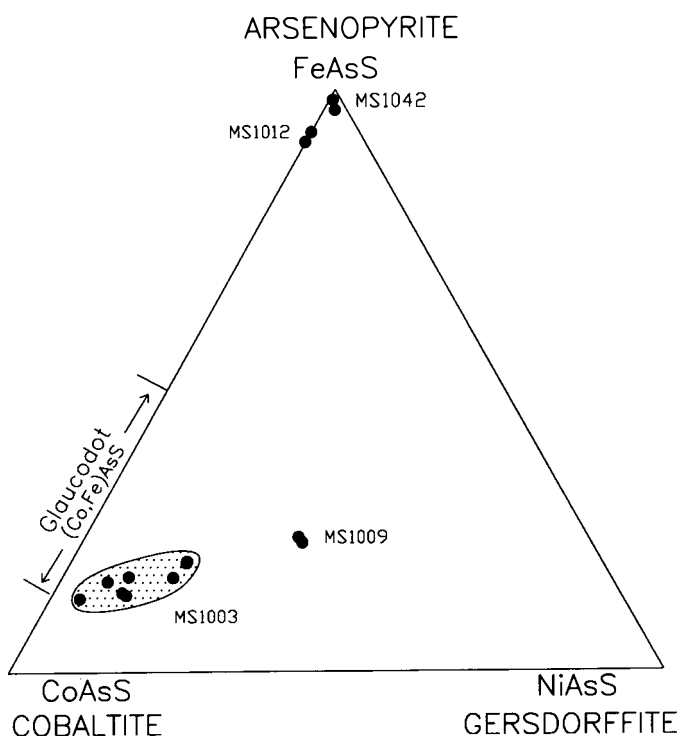

Fig. 6. Ternary diagram of arsenide compositions (atomic proportions) from metasedimentary rocks of the Meguma Group in the system FeAsS-CoAsS-NiAsS.

Co than Fe and the ratio of CoAsS:FeAsS may reach 6:1. In the analyzed sample the average CoAsS:FeAsS is 6:1.26.

Cobaltite was found only as an inclusion in a pyrite crystal in a sample of metasandstone from undivided Goldenville Formation (Table 1). The analyzed cobaltite is not chemically pure cobaltite (CoAsS), but rather (Co,Ni,Fe)AsS (Table 6). The atomic percentage of Co, Ni and Fe differ greatly from the previously described glaucodot. Composition of the analysed cobaltite plots closer to glaucodot than cobaltite on the same ternary diagram (Fig. 7), and thus this cobaltite likely reflects solid solution between cobaltite and gersdorffite (NiAsS) with anomalous Fe.

Chalcopyrite

Minor chalcopyrite occurs throughout the stratigraphic succession. Most of the chalcopyrite is found as inclusions within or in contact with pyrite or pyrrhotite. Grains vary in length from 1 mm to 5 mm and occur as anhedral blebs with no noticeable structure (e.g., Fig. 5g). Chalcopyrite accounts for <1% of the total sulphide minerals in any sample. Rare colloidal chalcopyrite in contact with pyrite was noted in 2 samples. Microprobe analyses are stoichiometrically $CuFeS_2$ (Table 7).

Covellite

One slate sample from the Cunard unit has covellite as a thin rim on chalcopyrite (average formula is $Cu_{0.99}F_{0.01}S$).

Table 5. Representative electron microprobe analyses of glaucodot.

Sample No.	MS1003	MS1003	MS1003
Unit	Beav(ub)[1]	Beav(ub)	Beav(ub)
Lithology	siltyslate	Siltyslate	Siltyslate
Position	1	2	3
wt.%			
Fe	4.74	4.66	5.65
As	44.14	43.93	45.34
S	20.27	20.60	19.34
Ni	3.28	2.83	5.44
Mn	0.30	0.22	0.72
Co	27.31	27.29	22.99
Bi	-	0.87	-
W	0.29	-	-
Total	100.33	100.40	99.48
at.%			
Fe	4.63	4.56	5.60
As	32.15	32.01	33.52
S	34.50	35.07	33.42
Ni	3.05	2.63	5.13
Mn	0.30	0.22	0.73
Co	25.29	25.28	21.60
Bi	-	0.23	-
W	0.09	-	-
Total	100.00	100.00	100.00

[1]Beav(ub) = upper beds of the Beaverbank unit

Table 6. Representative electron microprobe analyses of cobaltite.

Sample No.	MS1009	MS1009
Unit	Gold.[1]	Gold.
Lithology	Wacke	Wacke
Position	1A	1C
wt.%		
Fe	7.67	7.63
As	45.37	45.37
S	18.80	18.83
Ni	11.15	11.10
Co	15.21	15.24
Total	98.20	98.17
at.%		
Fe	7.72	7.69
As	34.07	34.08
S	32.99	33.05
Ni	10.69	10.64
Co	14.52	14.55
Total	100.00	100.00
Formula		
(Co,Fe,Ni)	1.00	0.99
As	1.03	1.03
S	1.00	1.00
Total	3.03	3.02

[1]Gold. = Goldenville Formation

Oxides

Ilmenite

Ilmenite is present throughout the succession, although not in all samples, ranging from less than 1% to as much as 8%. The majority of grains are idiomorphic, typically lath-like or elongate (Fig. 5h), and commonly oriented parallel to cleavage. A small proportion of ilmenite occur as blebs. All grains range in length from 0.5 mm to 5 mm. Ilmenite displays a similar relationship to cleavage as noted for chlorite and chloritoid porphyroblasts in the Glen Brook unit and generation 1 pyrrhotite, with cleavage zones wrapping around ilmenite grains, suggesting a pre- to syn-cleavage origin. Where ilmenite occurs as inclusions in garnet, the ilmenite inclusions are not oriented parallel to cleavage (Fig. 5h).

Microprobe data indicate extensive pyrophanite-ilmenite solid solution (ilmenite-dominated) (Fig. 7). The ilmenite analyses show an average stoichiometric composition of $(Fe_{0.76}Mn_{0.23})Ti_{0.98}O_3$ (Table 8), or calculated solid solution compositional average: $Pyr_{23}Ilm_{77}$. This indicates that the bulk composition of these samples was high in Mn. Ilmenite in its pure form, $FeTiO_3$, usually contains some $MnTiO_3$ and $MgTiO_3$ (Ramdohr, 1980). Craig and Vaughan (1979)
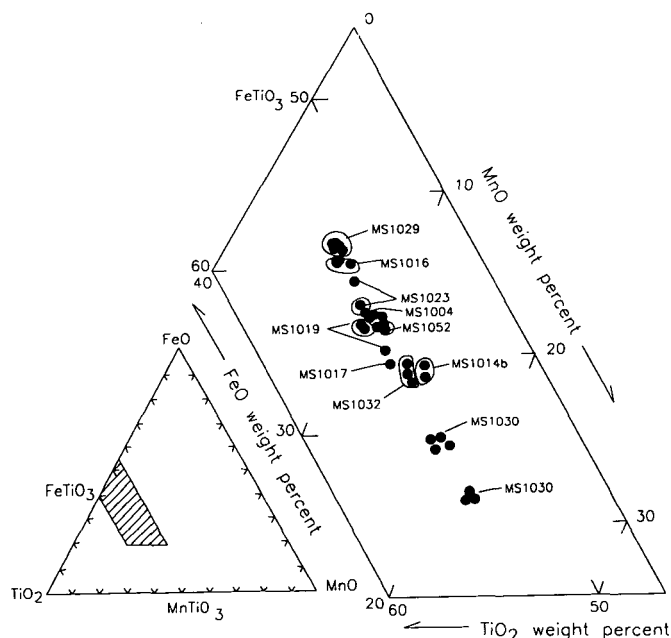

Fig. 7. Ternary diagram of ilmentite compositions (wt.%) from metasedimentary rocks of the Meguma Group in the system MnO-TiO_2-FeO.

Table 7. Representative electron microprobe analysis of chalcopyrite.

Sample No.	MS1032	MS1003	MS1041	MS1009
Unit	Cunard b	Beav(ub)[1]	Steves Rd.	Gold.[2]
Lithology	Slate	Siltyslate	Siltstone	Wacke
Position	1-41	4C	3-66	1D
wt.%				
Cu	35.09	33.01	34.00	34.01
Fe	30.88	30.31	29.67	30.12
S	35.06	34.44	34.71	34.50
Mn	-	0.65	-	-
Sb	-	-	0.22	-
Zn	-	-	1.45	-
W	-	0.30	0.20	-
Total	101.03	98.71	100.25	98.63
at.%				
Cu	25.11	24.16	24.61	24.89
Fe	25.14	25.25	24.44	25.08
S	49.74	49.97	49.80	50.03
Mn	-	0.55	-	-
Sb	-	-	0.08	-
Zn	-	-	1.02	-
W	-	0.08	0.05	-
Total	100.00	100.00	100.00	100.00
Formula				
Cu	1.01	0.97	0.99	1.00
Fe	1.01	1.01	0.98	1.00
S	2.00	2.00	2.00	2.00
Total	4.02	3.98	3.97	4.00

[1]Beav(ub) = upper beds of the Beaverbank unit
[2]Gold. = Goldenville Formation

suggested that the formula of ilmenite is better expressed as $(Fe,Mg,Mn)TiO_3$ due to extensive solid solution between ilmenite and geikielite (up to 70 mol per cent $MgTiO_3$) and between ilmenite and pyrophanite (up to 64 mol per cent $MnTiO_3$). Our calculated solid solution ranges from 10.96 mol per cent $MnTiO_3$ to 44.24 mol per cent $MnTiO_3$, which falls within the solid solution maximum for ilmenite suggested by Craig and Vaughan (1979). Limited data do not suggest any stratigraphic control on the Mn content of ilmentite (Table 8; Haysom, 1994) and range from 14.19% Mn (n=1) in the Goldenville Formation, 9.99% Mn (n=1) in the Beaverbank unit (although Feetham et al. (1997) reported 15.94% Mn), 10.08 to 21.18% Mn (n=3) in the Cunard unit, and 5.18 to 12.21% (n=3) in the Glen Brook unit. The most notable variation is the generally lower Mn content in ilmenite from the Glen Brook unit.

Rutile and anatase

Rutile was noted throughout the succession, occurring as euhedral laths or thin needles, most of which show well defined polysynthetic twins. Concentrations range from <1% to about 2%. The grains do not appear to be the result of replacement.

Anatase is the most common titanium oxide in slate and metasandstone of the Rawdon area, with a modal concentration of <1% to 4%. Anatase crystals are anhedral to subhedral, and occur in fine grained aggregates that are in contact with or inside sulphide minerals. In samples containing both anatase and ilmenite, 25% of ilmenite grains are partially replaced by anatase. The anatase in the rocks of the area thus either mantled pyrrhotite or replaced ilmenite. Microprobe data for both polymorphs (rutile and anatase) does not discriminate them. All data for TiO_2 polymorphs show elevated levels of Fe; FeO values average 0.5 wt.% and reach as high as 1.9 wt.% (Haysom, 1994).

Magnetite

Magnetite was found only in metasandstone samples from the Goldenville Formation and only two of the samples (Table 9) contain more than 5% magnetite. It occurs as subhedral to euhedral grains with interlocking grain boundaries, suggesting a metamorphic, rather than detrital, origin. The relative age of magnetite is difficult to determine as cleavage and strain are not evident either in hand specimen or thin section.

PARAGENESIS

1. Early diagenesis

The rocks studied have undergone regional deformation and metamorphism and thus any early diagenetic minerals have not been preserved. However, certain parts of the diagenetic history can be interpreted. The manganese-rich character of the Beaverbank unit and the sulphide- and carbon-rich character of the Cunard unit have been interpreted by Waldron (1992) and Schenk (1991) to reflect anoxic conditions, which promote the reduction of seawater sulphate and manganese oxide. Waldron (1992) suggested that manganese oxide generated at the reducing-oxidizing boundary was concentrated as Mn-carbonate within the Beaverbank unit during early diagenesis under reducing conditions. During early diagenesis of sediment, pore water sulphate was reduced to sulphide, which combined with iron to form pyrite. The reduction process is driven by organic carbon, which is particularly abundant in the black slates of the basal Halifax Formation (maximum values of 3 to 10%: Graves and Zentilli, 1988, Sangster, 1990). Waldron (1992) interpreted sulphur isotopes (Sangster, 1990) to indicate diagenesis of the Moshers Island member (Beaverbank unit of this study) in an environment open to seawater sulphate, whereas diagenesis of the Cunard Member occurred either in a closed system separated

Table 8. Representative electron microprobe analyses of ilmenite.

Sample No.	MS1030	MS1030	MS1023	MS1029	MS1019	MS1014b
Unit	Cunard b	Cunard b	Glen Bk.	Glen Bk.	Cunard b	Gold.[1]
Lithology	Slate	Slate	Slate	Slate	Slate	Wacke
Position	1-A138	3-A147	2-A104	1-A131	A85	1-A46
wt.%						
SiO_2	0.13	0.14	0.24	-	0.35	0.26
TiO_2	52.67	52.87	51.92	52.94	52.04	51.13
FeO_t	29.87	26.45	38.54	41.71	34.87	33.86
MnO	16.62	20.49	7.68	5.33	11.64	14.17
Total	99.29	99.95	98.38	99.98	98.90	99.42
Formula						
(Fe,Mn)	0.99	0.99	0.99	0.99	0.99	1.03
Ti	1.00	1.00	1.00	1.00	0.99	0.98
O	3.00	3.00	3.00	3.00	3.00	3.00
Total	4.99	4.99	4.99	5.00	4.98	5.01

[1]Gold. = Goldenville Formation

Table 9. Representative electron microprobe analyses of magnetite.

Sample No.	MS1011	MS1011	MS1014b	MS1014b
Unit	Gold.[1]	Gold.	Gold.	Gold.
Lithology	Wacke	Wacke	Wacke	Wacke
Position	3-A59	3-A61	1-A44	1-A47
wt.%				
SiO_2	-	0.16	0.19	0.25
FeO_t	94.05	93.63	93.20	93.75
Cr_2O_3	0.29	0.22	-	0.18
V_2O_5	0.25	0.32	--	-
Total	94.59	94.33	93.39	94.18

[1]Gold. = Goldenville Formation

from seawater or in an isolated basin. Although changes in oxygen levels in bottom water may have influenced pyrite abundance (Schenk, 1991; Waldron, 1992), it is possible that the sands of the Goldenville Formation contained less detrital iron and less organic carbon, thus producing less pyrite than in the Beaverbank unit.

Rutile also appears to be an early diagenetic mineral, as rutile paragenesis under metamorphic conditions is typically associated with temperatures >600°C and there is no evidence for such high temperatures in the study area. Deer *et al.* (1974) suggested that rutile may form thin needle-like crystals at low temperatures during the reconstitution process in shales. Such an early diagenetic origin thus appears to be more probable for formation of rutile in our samples.

2. Pre- or syn-cleavage prograde metamorphism

Evidence presented above indicates a similar paragenetic relationship with respect to cleavage for generation 1 pyrrhotite, ilmenite and porphyroblastic chlorite and chloritoid, and all are interpreted to have formed during regional metamorphism and deformation. Generation 1 pyrrhotite clearly predated cleavage-related strain, whereas generation 2 pyrrhotite has little cleavage-related strain and contains inclusions of cleavage-parallel muscovite, indicating a post-cleavage age. The fact that all pyrrhotite is chemically similar suggests that the two generations may be part of a continuous episode of pyrrhotite formation over an extended period of cleavage development during regional deformation and metamorphism.

Ferry (1981) described a metamorphic reaction ($2FeS_2$ + $2H_2O$ + C = 2FeS + $2H_2S$ + CO_2) that produces pyrrhotite by desulfidation of pyrite during prograde metamorphism. The Meguma Group appears to have contained sufficient metamorphic fluids and had low enough oxygen fugacity for the conversion of pyrite to pyrrhotite to go to completion, as no early diagenetic pyrite has been recognized. Anatase mantles pyrrhotite throughout the sulphide-rich slates. Excess TiO_2 was generated during diagenesis from ilmenite and pyrophanite. Thus, the fluids responsible for pyrrhotite formation were rich in Ti and anatase (TiO_2) may have formed from the remaining excess fluids after pyrrhotite genesis.

Garnet probably was formed after pyrrhotite and ilmenite, because the garnet surrounds pyrrhotite grains and inclusions of ilmenite are found within the garnet crystals. The garnet and ilmenite crystals are rich in manganese and iron, likely due to Mn- and Fe-rich metamorphic fluids derived from the manganese-rich Beaverbank unit. The solid solu-

tion between Mn-rich pyrophanite and Fe-rich ilmenite, and the solid solution between Mn-rich spessartine and Fe-rich almandine metamorphic reaction is as follows: $1/3 Fe_3Al_2Si_3O_{12}$ + $MnTiO_3$ = $1/3Mn_3Al_2Si_3O_{12}$ + $FeTiO_3$ (almandine + pyrophanite = spessartine + ilmenite).

During prograde metamorphic reactions, fluids concentrated Co, Fe, and Ni to form the Co-Fe-Ni-rich arsenides (glaucodot and cobaltite) in samples from the Beaverbank unit and upper Goldenville Formation. This enrichment is only local and not observed throughout all the samples of the Rawdon area. Ixner *et al.* (1979) have determined experimentally the solid solution limits of the Co, Fe, Ni sulpharsenide ternary system. In such a plot, the required temperature for our chemical composition is >500°C. However, the metamorphic conditions in the Meguma Group metasedimentary rocks only reached chlorite-grade greenschist facies (200 to 400°C). Thus, the experimental solid solution limits of Ixner *et al.* (1979) appear inappropriate for the Meguma Group, perhaps because of different fluid conditions. Fleet and Burns (1990) described a cobaltite from Sudbury, Ontario, that is very similar to the analysis from our sample and they also considered it as a cobaltite-gersdorffite solid solution.

Cleavage developed after this initial metamorphic mineralization and formed well developed planes which bend around pyrrhotite, ilmenite and garnet grains. Some pyrrhotite which partially overprinted the cleavage formed during the end of the progressive metamorphism.

3. Retrograde metamorphism and secondary reactions due to fluid migration

All pyrite postdates pyrrhotite and, in most cases, pyrite clearly resulted from retrograde metamorphic reactions involving the oxidation of pyrrhotite and subsequent formation of pyrite. The reaction is as follows (Hall and Fallick, 1988):

$$8FeS + 5CO_2 + 2H_2O = 4FeS_2 + CH_4 + 4FeCO_3$$
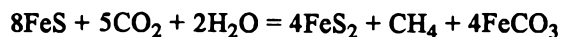
Partial to complete replacement of pyrrhotite lenses by colloform or birds-eye pyrite (Type 1) appears to postdate cleavage. Hall *et al.* (1987) have described similar pyrite porphyroblasts and conclude that they formed from disseminated pyrrhotite. Pyrite stringers branching off from Type 1 pyrite lenses provide evidence of limited transport. Mobilization of this pyrite locally has almost completely destroyed the primary pyrite replacement porphyroblasts and only fine grained skeletal pyrite with an internal quartz core remains (Fig. 5e). Close to such porphyroblasts a pyrrhotite-free zone (depletion zone) contains quartz that replaced the early pyrrhotite. Thus the quartz core in Figure 5e might have replaced the Type 1 pyrite porphyroblasts which consequently have been used to form the Type 2 pyrite (cubes).

Amorphous colloidal chalcopyrite is found always in contact with pyrite and pyrrhotite. Arsenopyrite crystals formed as euhedral crystals within sulphide minerals. Both of these minerals formed as late-stage replacement products of the pyrite and/or pyrrhotite.   •

Ramdohr (1980) noted that a rather common reaction between titaniferous minerals and iron occurs in ore-bearing solutions. Iron ores first precipitate from solution and the titanium component in the solution precipitates as TiO_2. Anatase, which replaces ilmenite as a fine grained aggregate (Haysom, 1994; Plate 16), formed after prograde metamorphism, at which time ilmenite was formed. Replacement of ilmenite by rutile has also been described by Ramdohr (1980), where rutile, in many cases, originated from ilmenite by hydrothermal processes. The oxidation reaction is as follows: $2FeTiO_3 + 1/2O_2 = Fe_2O_3 + 2TiO_2$.

CONCLUSIONS

(1) A strong stratigraphic control of opaque minerals in the Meguma Group probably reflects initial conditions of sedimentation. Identification of opaque minerals and their distribution and concentration is important for evaluation of environmental hazards such as acid drainage.

(2) Pyrite formed, particularly in carbon-rich black shales, during early diagenesis, although no early pyrite is preserved. Rutile may also be an early diagenetic mineral.

(3) Pyrrhotite and ilmenite developed under regional prograde metamorphic conditions and during cleavage formation, contemporaneously with porphyroblastic growth of garnet, chlorite and chloritoid. Local formation of glaucodot and cobaltite also occurred at this time.

(4) Pyrite preserved in the rocks of the study area formed during retrograde metamorphism by the breakdown of pyrrhotite to form colloform and bird's-eye pyrite and pyrite aggregates and by remobilization of type one pyrite to form pyrite cubes. Arsenopyrite and chalcopyrite also appear to be late-stage minerals.

ACKNOWLEDGEMENTS

BINNEY, W.P., JENNER, K.A., SANGSTER, A.L., and ZENTILLI, M. 1986. A stratabound zinc-lead deposit in Meguma Group metasediments at Eastville, Nova Scotia. Maritime Sediments and Atlantic Geology, 22, pp. 65-88.

CRAIG, J.R. and VAUGHAN, D.J. 1979. Mineral chemistry of metal sulfides. Cambridge University Press, Cambridge, England.

DEER, W.A., HOWIE, R.A., and ZUSSMAN, J. 1974. An introduction to the rock-forming minerals. Longman Group Limited, London.

ERSLEV, E.A. and WARD, D.J. 1994. Non-volatile element and volume flux in coalesced slaty cleavage. Journal of Structural Geology, 16, pp. 531-553.

FARIBAULT, E.R. 1908. Elmsdale sheet. Geological Survey of Canada, Map No. 66, Publication No. 1005.

FEETHAM, M., RYAN, R.J., PE-PIPER, G., and O'BEIRNE-RYAN, A.M. 1997. Lithogeochemical characterization of the Beaverbank unit of the Halifax Formation and acid drainage implications. Atlantic Geology, 33, pp. 133-141.

FERRY, J.M. 1981. Petrology of graphitic sulfide-rich schists from south-central Maine: an example of desulfidation during prograde regional metamorphism. American Mineralogist, 66, pp. 908-930.

FLEET, M.E. and BURNS, P.C. 1990. Structure and twinning of cobaltite. Canadian Mineralogist, 28, pp. 719-723.

FLETCHER, H. and FARIBAULT, E.R. 1911. Southeast Nova Scotia. Canada Department of Mines, Geological Survey, Map 53a, scale 1:250 000.

FOX, D.L. 1994. Geological mapping in the Upper Rawdon-Ardoise area, Hants County, Nova Scotia. In Program and Summaries, Eighteenth Annual Review of Activities. Edited by D.R. MacDonald. Nova Scotia Department of Natural Resources, Mines and Energy Branches Report 94-2, p. 21.

FUETEN, F. 1984. Spaced cleavage development in the metagreywackes of the Goldenville Formation, Meguma Group, Nova Scotia. Unpublished M.Sc. thesis, McMaster University, Hamilton, Ontario, Canada.

GRAVES, M.C. and ZENTILLI, M. 1988. The lithogeochemistry of metal-enriched coticules in the Goldenville-Halifax transition zone of the Meguma Group, Nova Scotia. Geological Survey of Canada, Paper 88-1B, pp. 251-261.

HALL, A.J. and FALLICK, A.E. 1988. A sulphur isotope study of iron sulphides in the late Precambrian Dalradian Easdale Slate Formation, Argyll, Scotland. Mineralogical Magazine, 52, pp. 483-490.

HALL, A.J., BOYCE, A.J., and FALLICK, A.E. 1987. Iron sulphides in metasediments: isotopic support for a retrogressive pyrrhotite to pyrite reaction. Chemical Geology, 65, pp. 305-310.

HAYSOM, S.J. 1994. The opaque mineralogy, petrology, and geochemistry of the Meguma Group metasediments, Rawdon area, Nova Scotia. Unpublished B.Sc. thesis, St. Mary's University, Halifax, Nova Scotia.

HENDERSON, J.R., WRIGHT, T.O., and HENDERSON, M.N. 1986. A history of cleavage and folding: An example from the Goldenville Formation, Nova Scotia. Geological Society of America Bulletin, 97, pp. 1354-1366.

HORNE, R.J. 1993. Preliminary report of the geology of the Rawdon area. In Mines and Energy Branch Report of Activities 1992. Edited by D.R. MacDonald and K.A. Mills. Nova Scotia Department of Natural Resources, Mines and Energy Branches, Report 93-1, pp. 61-67.

----- 1995. Update on bedrock mapping of the Rawdon Syncline. In Mines and Energy Branch Report of Activities 1994. Edited by D.R. MacDonald and K.A. Mills. Nova Scotia Department of Natural Resources, Mines and Minerals Branch Report 95-1, pp. 57-61.

HORNE, R.J. and CULSHAW, N. 1994a. Preliminary evaluation of flexural slip and its significance in localizing auriferous veins in the Meguma Group, Nova Scotia. In Mines and Minerals Branch Report of Activities 1993. Edited by D.R. MacDonald.

Nova Scotia Department of Natural Resources, Mines and Mineral Branches Report 94-1, pp. 147-160.

----- 1994b. Central Meguma project: Progress report on structural studies. In Program and Summaries, Eighteenth annual review of activities. Edited by D.R. MacDonald. Nova Scotia Department of Natural Resources, Mines and Minerals Branches Report 94-2, p. 19.

IXNER, R.A., STANLEY, C.J., and VAUGHAN, D.J. 1979. Cobalt-, nickel-, and iron-bearing sulpharsenides from the North of England. Mineralogical Magazine, 43, pp. 389-395.

JENNER, K. 1982. A study of sulfide mineralization in Gold Brook, Colchester County, Nova Scotia. Unpublished B.Sc. thesis, Dalhousie University, Halifax, Nova Scotia.

KEPPIE, J.D. 1979. Geological map of Nova Scotia. Nova Scotia Department of Mines and Energy map, scale 1:500 000.

KEPPIE, J.D. and DALLMEYER, R.D. 1987. Dating transcurrent terrane accretion: an example from the Meguma and Avalon composite terranes in the northern Appalachians. Tectonics, 6, pp. 831-847.

KEPPIE, J.D. and MUECKE, G.K. 1979. Metamorphic map of Nova Scotia. Nova Scotia Department of Mines and Energy map, scale 1:1 000 000.

KING, M.S. 1994. Magnetic mineralogy and susceptibility of the north-central Meguma Group: implications for the interpretation of aeromagnetic total field, first derivative and second derivative. Nova Scotia Department of Natural Resources, Open File Report 94-004.

----- 1995. Interpretation of magnetic data from the Meguma Group of Nova Scotia: Magnetic mineralogy. In Mines and Energy Branch Report of Activities 1994. Edited by D.R. MacDonald and K.A. Mills. Nova Scotia Department of Natural Resources, Mines and Minerals Branch Report 95-1, pp. 63-72.

KNEE, K. 1995. Magnetic susceptibility of Halifax Formation slates at the Halifax International Airport: correlation with potential for acid drainage. Unpublished B.Sc thesis, Dalhousie University, Halifax, Nova Scotia.

MACINNIS, I.N. 1986. Lithogeochemistry of the Goldenville-Halifax transition (GHT) of the Meguma Group in the manganiferous zinc-lead deposit at Eastville, Nova Scotia. Unpublished B.Sc. thesis, Dalhousie University, Halifax, Nova Scotia.

MUECKE, G.K., ELIAS, P., and REYNOLDS, P.H. 1988. Hercynian/ Alleghanian overprinting of an Acadian Terrane: $^{40}Ar/^{39}Ar$ studies in the Meguma Zone, Nova Scotia, Canada. Chemical Geology, 73, pp. 153-167.

O'BRIEN, B. 1988. A study of the Meguma Terrane in Lunenburg County, Nova Scotia. Geological Survey of Canada, Open File Report 1823.

RAMDOHR, P. 1980. The ore minerals and their intergrowths. Pergamon Press, Oxford.

RYAN, R.J. 1994. Preliminary Investigations of Meguma Group stratigraphy in the Beaverbank area, Nova Scotia. In Mines and Mineral Branch, Report of Activities 1993. Edited by D.R. MacDonald. Nova Scotia Department of Natural Resources, Mines and Minerals Branch Report 94-1, pp. 137-140.

RYAN, R.J., FOX, D., HORNE, R.J., COREY, M.C., and SMITH, P.K. 1996. Preliminary stratigraphy of the Meguma Group in central Nova Scotia. In Minerals and Energy Branch, Report of Activities 1995. Edited by D.R. MacDonald and K.A. Mills. Nova Scotia Department of Natural Resources, Mines and Minerals Branch Report 96-1, pp. 27-34.

SANGSTER, A.L. 1990. Metallogeny of the Meguma Terrane, Nova Scotia. In Mineral deposit studies in Nova Scotia, Volume I. Edited by A.L. Sangster. Geological Survey of Canada Paper 90-8, pp. 115-162.

SCHENK, P.E. 1991. Events and sea-level changes on Gondwana's margin; The Meguma Zone (Cambrian to Devonian) of Nova Scotia, Canada. Geological Society of America Bulletin, 103, pp. 512-521.

SCHWARZ, E.J. and BROOM, J. 1994. Magnetic anomalies due to pyrrhotite in Palaeozoic sediments in Nova Scotia, Eastern Canada. Journal of Applied Geophysics, 32, pp. 1-10.

TREAGUS, S.H. 1988. A history of cleavage and folding: an example from the Goldenville Formation, Nova Scotia: Discussion and Reply. Geological Society of America Bulletin, 100, pp. 152-154.

WALDRON, J.W.F. 1992. The Goldenville-Halifax transition, Mahone Bay, Nova Scotia: relative sea-level rise in the Meguma source terrane. Canadian Journal of Earth Sciences, 29, pp. 1091-1105.

WILLIAMS, P.F., GOODWIN, L.B., and LAFRANCE, B. 1995. Brittle faulting in the Canadian Appalachians and the interpretation of seismic data. Journal of Structural Geology, 17, pp. 215-232.

WOODMAN, J.E. 1904. The sediments of the Meguma Series of Nova Scotia. The American Geologist, 34, pp. 14-34.

WRIGHT, T.O. and HENDERSON, J.R. 1992. Volume loss during slaty cleavage formation in the Meguma Group, Nova Scotia, Canada. Journal of Structural Geology, 14, pp. 281-290.

ZENTILLI, M., GRAVES, M.C., MULJA, T., and MACINNIS, I. 1986. Geochemical characterization of the Goldenville-Halifax transition of the Meguma Group of Nova Scotia: preliminary report. In Current Research, Part A. Geological Survey of Canada, Paper 86-1A, pp. 423-428.